Geosynchronous patrol orbit for space situational awareness

Blair Thompson, Thomas Kelecy, Thomas Kubancik
Applied Defense Solutions

Tim Flora, Michael Chylla, Debra Rose
Sierra Nevada Corporation

ABSTRACT

Applying eccentricity to a geosynchronous orbit produces both longitudinal and radial motion when viewed in Earth-fixed coordinates. An interesting family of orbits emerges, useful for "neighborhood patrol" space situational awareness and other missions. The basic result is a periodic (daily), quasi-elliptical, closed path around a fixed region of the geosynchronous (geo) orbit belt, keeping a sensor spacecraft in relatively close vicinity to designated geo objects. The motion is similar, in some regards, to the relative motion that may be encountered during spacecraft proximity operations, but on a much larger scale. The patrol orbit does not occupy a fixed slot in the geo belt, and the east-west motion can be combined with north-south motion caused by orbital inclination, leading to even greater versatility. Some practical uses of the geo patrol orbit include space surveillance (including catalog maintenance), and general space situational awareness. The patrol orbit offers improved, diverse observation geometry for angles-only sensors, resulting in faster, more accurate orbit determination compared to simple inclined geo orbits. In this paper, we analyze the requirements for putting a spacecraft in a patrol orbit, the unique station keeping requirements to compensate for perturbations, repositioning the patrol orbit to a different location along the geo belt, maneuvering into, around, and out of the volume for proximity operations with objects within the volume, and safe end-of-life disposal requirements.

1. INTRODUCTION

The traditional geosynchronous ("geosynch" or "geo") orbit is designed to keep a spacecraft in a nearly fixed position (longitude, latitude, and altitude) with respect to the rotating Earth. The longitude is often assigned by international agreement, latitude is kept near zero, and the altitude of the geosynch orbit is a function of orbital mechanics [1]. A non-zero orbital inclination gives the orbit and ground tracks a periodic north-south motion, repeating approximately once per day. An example of this type of motion is the classic "figure of eight" ground track of a circular, inclined geo orbit [1]. Similarly, introducing eccentricity to a geosynch orbit causes once-per-orbit (or per-revolution, "per-rev") altitude and longitudinal variations in the orbit track. The result, when viewed in Earth-fixed coordinates, is a periodic, quasi-elliptical, closed-path trajectory that appears to orbit or "fly around" a fixed region of the geo belt (e.g., Fig. 1). Once established, the quasi-elliptical relative motion is natural for all time – no active thrusting is required (barring possible station keeping requirements, cf. §4). This type of orbit is called a *patrol orbit* because the spacecraft remains in the vicinity of a designated section of the geo belt with continuous relative motion. It is patrolling a section of the geo belt analogous to a "neighborhood patrol" program on Earth. A spacecraft in a patrol orbit is well poised to provide observation of (and perhaps "assistance" to) objects in its geo "neighborhood" as needed. Furthermore, a spacecraft in a patrol orbit does not occupy any fixed "slot" in the geo belt, and (with inclination) crosses the equator at an altitude different than the nominal geo belt, significantly reducing collision hazard.

The relative motion of the patrol orbit is conceptually similar to natural motion circumnavigation (NMC) of spacecraft proximity operations [2], but the underlying dynamics are fundamentally different. Unlike the relative motion of proximity operations and formation flying, the patrol orbit equations of motion are with respect to Earth and independent of

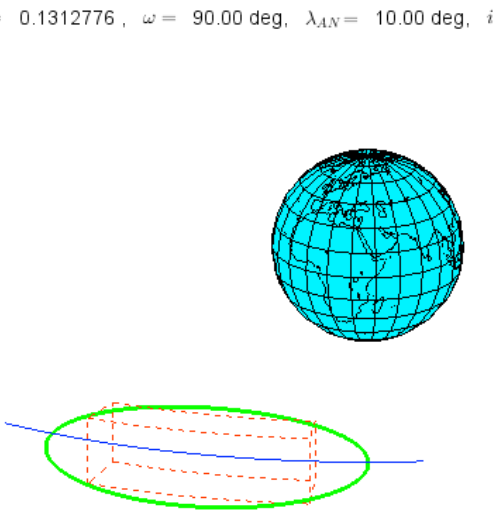

Fig. 1: Example $30^\circ \times 4^\circ$ patrol orbit (green) viewed in Earth-fixed coordinates.

the motion of any other orbiting object. Additionally, proximity operations typically occur at a range of perhaps tens of kilometers and less. This is often due to assumptions and limitations of the equations of relative motion (e.g., the Clohessy-Wiltshire (CW) equations [2]). On the other hand, a patrol orbit might cover tens of thousands of kilometers with no limitations on the equations of motion.

The patrol orbit offers several advantages over the traditional geosynch orbit, especially for space situational awareness (SSA) missions. The patrol orbit enables relatively close surveillance or inspection of resident space objects (RSO) within or near the neighborhood zone of interest, which also allows smaller sensors compared to Earth-bound sensors observing the same region of the geo belt. Observation from a patrol orbit guarantees that observation ranges will fall within pre-specified limits, meeting sensor payload requirements. Observation of geo objects from a patrol orbit also results in greater angular viewing diversity over time and allows observation of an object from multiple viewing angles, which is especially significant for imaging missions. Furthermore, patrol orbits are not affected by terrestrial weather conditions and are not restricted to nighttime only observation. A patrol orbit may also serve as a convenient launching point for a sub-satellite (i.e., CubeSat) for rendezvous and servicing or close "flyby" inspection of geo RSO's. This mission set might be extended to geo debris removal or dealing with an uncontrollable or rogue spacecraft. A constellation of spacecraft in multiple patrol orbits or phased in the same patrol orbit could also expand mission capabilities.

An example patrol orbit is shown in Fig.1 (in green). The corresponding orbital elements are listed in Table 1. Also shown in the figure is an example *patrol zone* (in dashed red). The patrol zone is a volume of interest – the "neighborhood" – defined by specific SSA mission requirements. In this case, the example patrol zone is from -3° to $+3^\circ$ latitude, 15° to 35° longitude, and $\pm 2,000$ km altitude from the nominal geo belt, a local section of which is also shown in Fig.1 (5° to 45° longitude, in blue). The node-to-node longitude separation of the example patrol orbit is 30°, and the orbit track covers a 4° latitude range ($\pm 2^\circ$ centered on the geo belt). This orbit is referred to as a $30^\circ \times 4^\circ$ patrol orbit and is the baseline example used for analysis in this paper. The argument of perigee (ω) is 90°, putting perigee at the farthest northern point on the orbit track. The ascending node of the orbit is on the western end of the orbit track (to the left in the figure). From the perspective of Fig.1, the spacecraft will appear to move clockwise along the patrol orbit – traveling faster than the Earth's rotation on the northern side of the orbit, slower on the southern side. Although not obvious from Fig.1, the patrol orbit does not lie in a flat plane when viewed in Earth-fixed coordinates – it is "warped" primarily along the major axis of the quasi-ellipse.

When considering patrol orbits it is important to distinguish between two frames of reference: Earth Centered Inertial (ECI) and Earth Centered Earth Fixed (ECEF). ECI is an inertial frame centered on the Earth and (nearly) fixed with respect to the distant background stars. This is the frame normally used for the orbital equations of motion and for quantifying orbital states in astrodynamics. ECEF is a non-inertial frame centered on and rotating with the Earth (i.e.,

Table 1: Orbital elements of the $30^\circ \times 4^\circ$ baseline patrol orbit shown in Fig. 1.

Epoch	20170710 12:00:00.000 UTC
a: semimajor axis	42164172.921 m
e: eccentricity	0.1312776
i: inclination	2°
Ω: RA of ascending node	118.603775°
ω: argument of perigee	90°
ν: true anomaly	270°
GMST: Greenwich Mean Sidereal Time	7h 14m 24.91s = 108.603775°
λ_{AN}: longitude of ascending node	10°
λ_{DN}: longitude of descending node	40°
Time from ascending to descending node	43081.522 sec

geosynchronous). It is convenient for geosynch orbital analysis because it is a geosynch frame. Visualizing relative motion in ECEF aids in understanding the value of patrol orbits for geo inspection and surveillance.

The remainder of the paper examines the observation properties of the baseline patrol orbit (§2), and quantitatively examines the patrol orbital elements (§3), station keeping requirements (§4), and maneuvering to and from the patrol orbit (§5). Finally, §6 examines the use of a currently existing spacecraft bus (the Sierra Nevada Corporation SN-200G) for use in a patrol orbit.

2. SSA APPLICATION – OBSERVING THE GEO BELT

2.1. Geo Belt Surveillance

The non-zero eccentricity and inclination of the baseline patrol orbit result in some potentially unique surveillance and rendezvous opportunities for objects in and around certain areas of the geo belt in the neighborhood of the patrol orbit satellite. This allows for a diversity of geometry, viewing and lighting conditions not afforded by a strictly low eccentricity and inclination surveillance satellite platform. The mission types can be broken down into (at least) two classes: (1) tasking for geo belt surveillance and (2) rendezvous and proximity operations.

For the geo belt surveillance mission, the patrol satellite might carry an optical sensor for the purpose of tracking resident space objects (RSO's) in and near the geo belt. In this case, a number of constraints on the optical sensor may be limited from ground and strictly geo sensors. These include sun, moon and Earth exclusion zones dictated by the optics of the sensor, and the apparent magnitude of the RSO which is a function of the sensor detection sensitivity, range to the RSO from the optical sensor, and the sun-RSO-observer (phase) angle. Fig. 2 shows the Declination (Dec) vs. Right Ascension (RA) tracks of the 706 near-geo "candidate" objects that are currently in the Space Track catalog [3] and meet the viewing constraints. They are derived from line-of-site vectors between the baseline patrol orbit and each RSO, and are subject to the 30° sun exclusion and 15° moon and Earth exclusions of the sensor boresight with respect to those objects. The two "egg" shaped voids are outages due to the sensor exclusion constraints. The RSO candidates were also subject to a maximum visual magnitude constraint of 16 Mv, and the 24-hour observation frequency distribution of those candidate RSO's is shown in Fig. 3. Lastly, the ranges to these objects are shown in Fig. 4 and indicate most of the candidate RSO's are too far away (> 500 km) to allow resolved imaging with a typical sensor from the example baseline patrol orbit.

However, due to the unique attribute of the orbital parameters, there is a region of the geo belt that falls within a range of angles and distances such that the patrol orbit satellite will "orbit" an RSO that is near geostationary (zero eccentricity and inclination). This "orbit" is illustrated in Fig. 5 where the azimuth, elevation and range are computed over a 24 hour period for the patrol orbit satellite relative to a reference frame centered at a geosynchronous satellite (orbital reference frame). Additional features of the patrol orbit are presented in more detail in the subsequent sections of this paper.

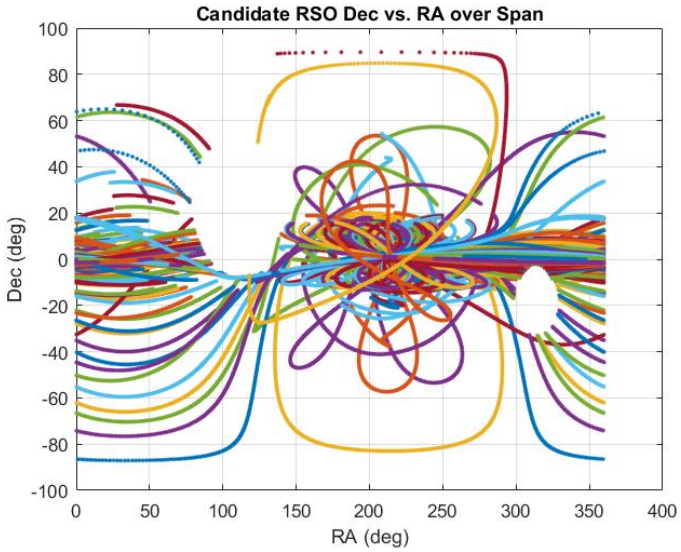

Fig. 2: Declination vs. Right Ascension of candidate geo RSO's from Space Track that are observable from the baseline patrol orbit.

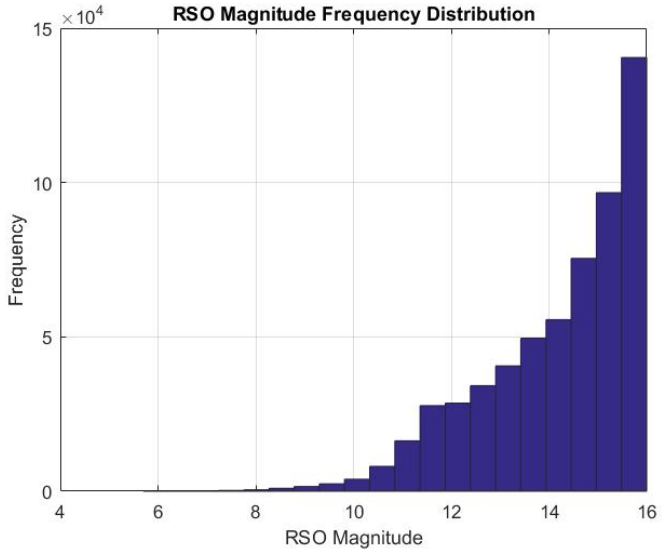

Fig. 3: Magnitude frequency distribution of candidate geo RSO's from Space Track that are observable from the baseline patrol orbit.

2.2. Viewing Geometry and Orbit Determination Accuracy

A simple simulation study was conducted to gauge the potential of the patrol orbit for improving geo RSO viewing geometry (i.e., angular diversity) over time compared to more traditional geo orbits. The goal of this study was to show *relative improvement* in orbit determination (OD) convergence time and accuracy, not the absolute OD accuracy achievable. The simulated observed RSO was in a circular, zero-inclination geo orbit at longitude $\lambda = 25^\circ$ (center of the patrol zone). Three sensor spacecraft made angles-only observations of the RSO from different geo orbits: (1) simple geostationary, (2) inclined circular geosynchronous ($i = 2^\circ$), and (3) the baseline patrol orbit. At sim start the sensor spacecraft were along the equator at $\lambda = 10^\circ$ (the ascending node of the patrol orbit). The spacecraft ECI states were numerically propagated using the two-body force model. Right ascension and declination observations were

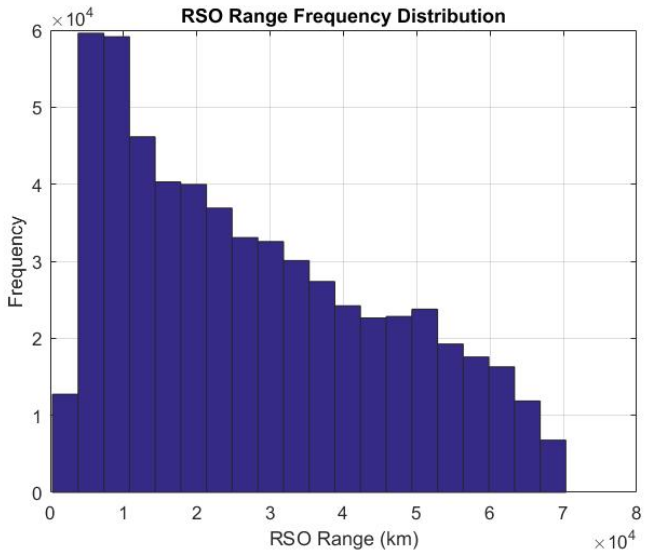

Fig. 4: Range frequency distribution of candidate geo RSO's from Space Track that are observable from the baseline patrol orbit.

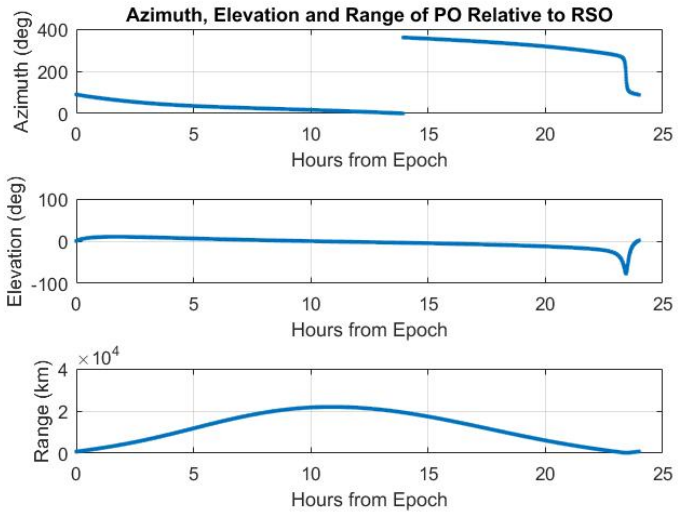

Fig. 5: Azimuth, Elevation and Range of the baseline patrol orbit satellite relative to an orbital reference frame centered at a geostationary satellite.

made by each sensor every 10 minutes for 24 hours, and zero-bias Gaussian observation noise ($\sigma = 3$ arcsec) was added. The effects of light propagation time were not modeled. Solar phase angle and exclusion were not considered. The observation data for each sensor were processed in an extended Kalman filter (EKF) using the classic form of the sequential filter equations [4]. The *a priori* state for each EKF was the "truth" state plus 10 km of error for each component of position and 10 m/s for each component of velocity. The *a priori* covariance was identical for all three EKF's. Process noise was not used in the EKF's, and there was no filter tuning performed.

The resulting position estimate errors vs. time are shown in Fig. 6. The simple geo sensor EKF converges at approximately 18 hours, the inclined geo EKF converges at approximately 10 hours, while the patrol orbit EKF converges at approximately 5 hours. With all initial conditions being nearly the same, the shorter convergence time can be at-

tributed (at least partially) to the more diverse viewing geometry of the patrol orbit. As always, discernment must

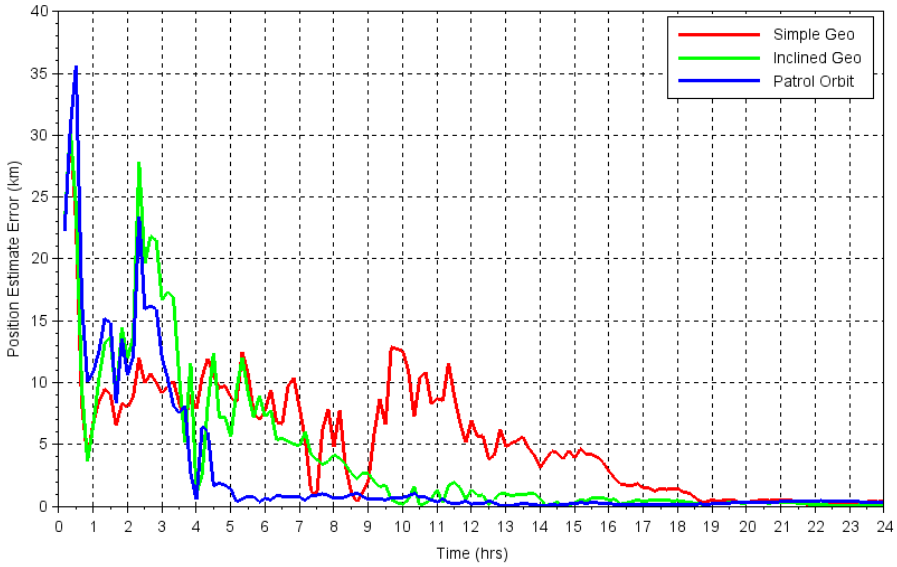

Fig. 6: Orbit determination study results.

be applied when considering these results – this was a single run of a simulation scenario using simplified dynamics, observation models, error models, etc. However, the results do suggest relative improvement in OD convergence time and accuracy, but additional high-fidelity simulation and study are in order, including covariance analysis.

Separate from the OD estimation problem, the 3-axis slew rate required to continuously track and observe the geostationary RSO from the baseline patrol orbit is shown in Fig. 7. The mean rate is approximately 0.002 deg/sec. The variation is caused by the continuously changing viewing geometry and orbital speed of the patrol orbit spacecraft. These slew rates are on par with slew rates of a traditional Earth-pointing geo spacecraft, but the implementation is a somewhat more complex due to the constantly changing slew rates involving all three spacecraft body axes. A gimbaled sensor could possibly deliver some (or most) of the required slew for one or two axes.

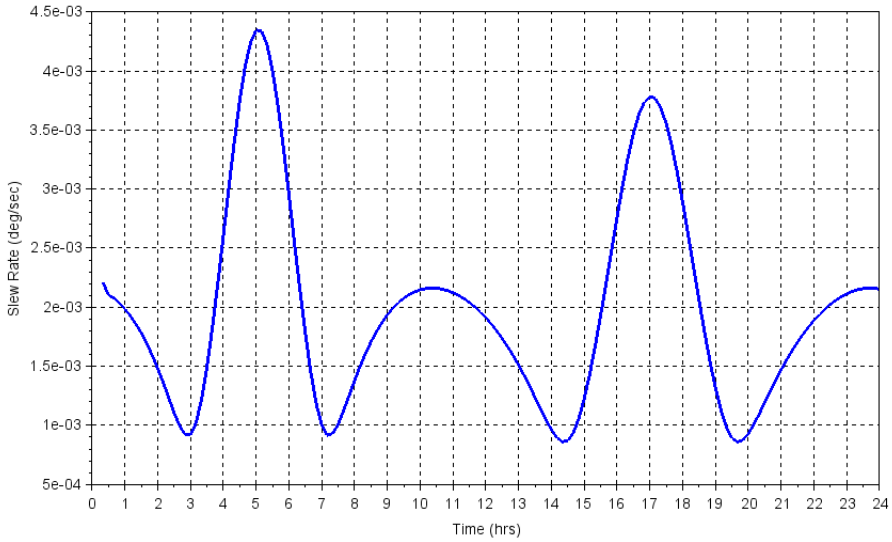

Fig. 7: 3-axis slew rate for tracking geostationary RSO at center of patrol zone. The mean rate is ≈ 0.002 deg/sec.

3. PATROL ORBIT PARAMETERS

The patrol orbit is most easily described and characterized in terms of the osculating (two-body) classical orbital elements [5]. The effects of perturbations are addressed in §4 in the context of station keeping requirements. Earth rotation is assumed uniform about the ECEF $\hat{z}$ axis at the constant rate of $\omega_\oplus$.

3.1. Semimajor Axis

The nominal patrol orbit is geosynchronous – its orbital period is equal to the rotational period of Earth (one sidereal day, $2\pi/\omega_\oplus \approx 23$hrs 56min 4.1sec). The nominal semimajor axis (a) is, therefore, a function of Earth's gravitational parameter (μ) and rotation rate $(\omega_\oplus)$

$$a = \left(\frac{\mu}{\omega_\oplus^2}\right)^{1/3} \approx 42,164,173 \text{ m} \tag{1}$$

The values

$$\begin{aligned} \mu &= 3.986004415 \times 10^{14} \text{ m}^3/\text{s}^2 \\ \omega_\oplus &= 7.292115 \times 10^{-5} \text{ rad/s} \end{aligned} \tag{2}$$

were used for the analysis presented in this paper. The nominal value of a is modified to compensate for certain perturbing forces (cf. §4) or to achieve other desired orbital characteristics such as asynchronous longitude drift (cf. §5.4). In particular, the change in a to effect change per rev in the longitude of the ascending node (λ_{AN}) is

$$\Delta a \approx \frac{\partial a}{\partial P}\left(-\frac{\Delta\lambda_{AN}}{\omega_\oplus}\right) = -\frac{\Delta\lambda_{AN}^\circ}{540\omega_\oplus}\sqrt{\frac{\mu}{a}} \tag{3}$$

where P is the orbital period $(P = 2\pi\sqrt{a^3/\mu})$. Note, for convenience, the far right-side form of (3) works on $\Delta\lambda_{AN}$ in degrees per rev. The equation can also be easily solved to compute $\Delta\lambda_{AN}^\circ$ for a given Δa.

3.2. Eccentricity and Argument of Perigee

As mentioned in the introduction, the eccentricity of the patrol orbit causes the periodic radial (altitude) and longitudinal (east-west) variations in the orbit track over the course of one orbital period when viewed in the ECEF frame. In general, the more eccentric the orbit the more radial and longitudinal variation occurs. The resulting longitude variation between the ascending node (AN) and descending node (DN) of the orbit – the nodal (node-to-node) variation in longitude $(\Delta\lambda_N)$ – is used as a defining parameter for a patrol orbit.

The nodal longitudinal variation is a result of the spacecraft traversing between the nodes (180° of true anomaly) with a time of flight different than what is required for the Earth to rotate 180°. If the orbit is circular there will be no longitudinal variation at the nodes (e.g., the classic "figure of eight" circular, inclined geo orbit track [1]). If the orbit has some eccentricity $(e \neq 0)$ the node-to-node traverse time will be different, although the overall orbital period will not change because it is a function of semimajor axis only. If the spacecraft passes through perigee going from AN to DN (i.e., $0 < \omega < 180^\circ$) it will arrive at the DN some time before Earth has rotated 180°, and the DN will be some point east of the AN in the equatorial plane. After one orbital period the spacecraft will be back at the AN, having formed a closed path relative to the geo belt (Fig. 1). It should be noted that a spacecraft will not travel along a patrol orbit uniformly with time – it will go faster near perigee and slower near apogee, as with any eccentric orbit.

To compute $\Delta\lambda_N$, the time from AN to DN must be known. The node-to-node time can be computed with two applications (two time periods) of Kepler's equation [5]. The first time period (t_1) is the time from AN to perigee. By virtue of time-of-flight symmetry about the perigee point, let $\nu = \omega$ then compute eccentric anomaly (E) using

$$E = \cos^{-1}\left(\frac{e + \cos\nu}{1 + e\cos\nu}\right) \tag{4}$$

A quadrant check on the inverse cosine function is not needed when considering cases $0 < \omega < 180°$. Kepler's equation is then used to compute time t_1 from

$$t = \frac{M}{n} = \sqrt{\frac{a^3}{\mu}}\,(E - e\sin E) \tag{5}$$

where n is the orbital mean motion $(n = \sqrt{\mu/a^3})$ and M is mean anomaly.

The second time period (t_2) is from perigee to the DN, completing the nodal traverse subject to the constraint $\omega + \nu = 180°$, or $\nu = 180° - \omega$. Time t_2 can be computed using (4) and (5). The total AN to DN time is $t_1 + t_2$. The nodal variation in longitude can then be computed as

$$\Delta\lambda_N^\circ = 180° - \frac{180°}{\pi}(t_1 + t_2)\omega_\oplus \tag{6}$$

The inverse problem, computing eccentricity given $\Delta\lambda_N$, appears to have no simple, direct solution. However, this is probably the more useful problem to solve for mission design and analysis purposes. Eccentricity vs. $\Delta\lambda_N$ for various ω computed numerically by *regula falsi* (e.g., [6]) are shown in Fig. 8. It is clear from the figure that for any $\Delta\lambda_N$ the required eccentricity is minimum when $\omega = 90°$. There also appear to be lower and upper limits to ω for a given $\Delta\lambda_N$. The function is quite linear for $\omega = 90°$, and a first-order approximation of eccentricity can be made using

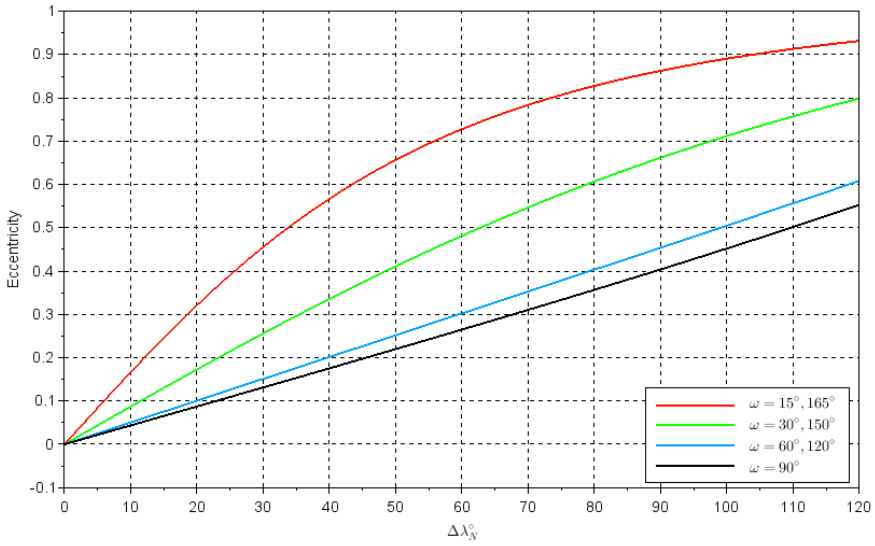

Fig. 8: Patrol orbit eccentricity vs. node-to-node $\Delta\lambda_N^\circ$ $(15° \leq \omega \leq 165°)$.

$$e \approx \frac{\Delta\lambda^\circ}{218.537} - 0.00582 \quad (\text{for } \omega = 90°) \tag{7}$$

Again, *regula falsi* or other numerical methods can be used to compute the precise value of eccentricity for a given $\Delta\lambda_N$ and any realizable value of ω.

The eccentricity of the patrol orbit ensures that the altitude will not be the nominal geo belt altitude at the nodes (i.e., equator crossings, $\nu = 90°$ and $270°$). Fig. 9 shows the altitude difference for patrol orbits with $\omega = 90°$. The altitude difference at the nodes can be computed from the polar form of the conic orbit equation [5] (with $\nu = 90°$)

$$\Delta r = a(1 - e^2) - a_{nom} \tag{8}$$

where a_{nom} is the nominal geo semimajor axis from (1). For the baseline patrol orbit of Table 1, the relative altitude at the nodes is -726.649 km. The Δr parameter is useful for assessing collision and conjunction hazards and interference with existing geo objects. Of course a patrol orbit with zero inclination $(i = 0°)$ will not have equator crossing nodes, but will cross the geo belt twice daily, leading to possible conjunction or collision conditions. This alone is a good reason to give the patrol orbit even a small amount of inclination.

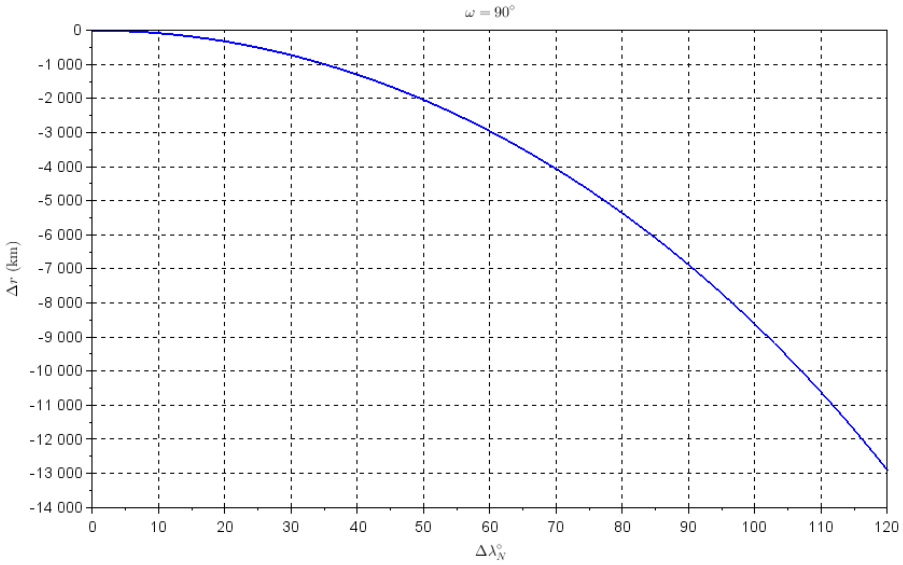

Fig. 9: Patrol orbit altitude at either node (equator crossing) relative to the nominal geo belt altitude $(\omega = 90°,\ \nu = 90°$ or $270°)$.

To a lesser extent, the argument of perigee also affects the east-west longitudinal variation of the patrol orbit track. This effect is related to the node-to-node traverse time as computed using (4) and (5). Several patrol orbits with the same semimajor axis and same eccentricity, but different argument of perigee, are shown in Fig. 10. In order to enclose the same patrol zone (red "box" in the figure), the longitude of the ascending node (λ_{AN}) must also be changed along with changing the argument of perigee. This property of patrol orbits will be exploited for passive east-west station keeping (cf. §4.2).

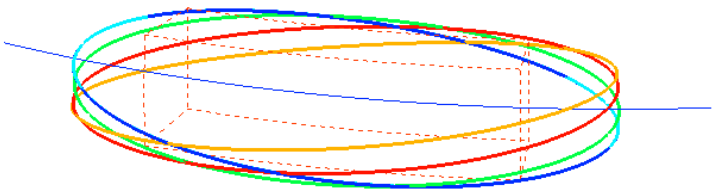

Fig. 10: Multiple patrol orbits enclosing same patrol zone: same semimajor axis and eccentricity, different argument of perigee and ascending node. See Fig. 12 for additional details.

Finally, it should be noted that if the argument of perigee is south of the equator (i.e., $180° < \omega < 360°$), the apparent relative motion of the spacecraft will be opposite to that of the baseline patrol orbit. The relative motion in Fig. 1 will appear to be clockwise because the spacecraft is traveling faster to the east near perigee, which is north of the equator $(\omega = 90°)$. The ascending node will be near the western end of the orbit track. A perigee that is south of

the equator (e.g., $\omega = 270^\circ$) will put the ascending node near the eastern end of the track. The orbit will be prograde (as is the baseline orbit), but the resulting relative motion will appear counterclockwise from the point of view of Fig. 1. There may be advantages to this opposing relative motion when designing constellations of patrol orbits, or when considering the resulting ground tracks for Earth observation and communications missions.

3.3. Inclination and Ascending Node

The inclination (i) and the right ascension of the ascending node (RAAN or Ω) completely specify the orientation of the orbital plane in inertial space (i.e., in the ECI frame). These two orbital elements are independent and have no effect on the longitudinal variation of the patrol orbit. As such, they are established based on other mission requirements. Inclination generally provides improved viewing geometry (cf. §2) and reduces collision hazard with geo objects (cf. §3.2), but may require additional maneuvering propellant, depending on orbit insertion conditions (cf. §5). As with all orbits, the inclination determines the maximum and minimum latitude of the orbit track (and ground track). Establishing the inclination to be one-half the longitudinal variation ($i = \Delta\lambda_N/2$) will result in quasi-circular orbit and ground tracks, although the patrol orbit will not be circular. The location of perigee will determine the direction of relative motion (cf. §3.2). The motion around the quasi-circular track will *not* be uniform in time due to the eccentricity of the patrol orbit.

The RAAN (Ω) is chosen to place the ascending node of the patrol orbit at the desired longitude as specified by SSA mission requirements. Longitude and right ascension are related by Greenwich sidereal time [5]. Therefore, the final value of Ω is established based on orbit and station insertion date and time.

4. STATION KEEPING – EFFECTS OF PERTURBATIONS

Although the nominal patrol orbit is geosynchronous, the effects of perturbations can be somewhat different compared to a traditional geosynchronous orbit. Consequently, the requirements and methods of station keeping are also somewhat different. This section explores the first-order effects of the major perturbing forces acting on the patrol orbit and strategies for mitigation.

4.1. Radial Compensation for Oblate Gravity

To first order, for an equatorial orbit $(i = 0^\circ)$, the J_2 zonal gravity of the oblate Earth manifests as excess point mass, independent of longitude. For an orbit to be geosynchronous, the radial distance (i.e., altitude) must be compensated for the apparent excess mass of the equatorial bulge. Substituting the radial acceleration from the spherical harmonic gravity model [7] into the two-body acceleration $(a = \mu/r^2)$ results in the recursive equation

$$r_{i+1} = \left\{ \frac{\mu}{\omega_\oplus^2} \left[1 - \frac{3}{2} \left(\frac{R_E}{r_i} \right)^2 C_{20} \right] \right\}^{1/3} \qquad i = 1, 2, 3 \tag{9}$$

where R_E is the Earth equatorial radius and C_{20} is the unitless second-degree gravity coefficient $(C_{20} = -J_2)$.

$$\begin{aligned} R_E &= 6378136.3 \text{ m} \\ C_{20} &= -J_2 = -0.00108263566655 \end{aligned} \tag{10}$$

The nominal value of a from (1) is used as the initial estimate of r_i. The equation converges very well in three iterations. The resulting r is ≈ 522.25 m higher than the nominal geo orbital radius. Equation (9) is for zero inclination and only includes J_2 gravity, but it provides a good starting point for designing a low-inclination patrol orbit.

The right ascension of the ascending node (Ω) of the baseline patrol orbit is expected to precess secularly due to J_2 gravity at a rate of [7]

$$\frac{d\Omega}{dt} = \frac{3nC_{20}R_E^2}{2(1-e^2)^2a^2} \cos i = -0.0138418 \text{ deg/rev} \tag{11}$$

where n is orbital mean motion ($n = \sqrt{\mu/a^3}$). This precession of the nodes can be nulled by changing the semimajor axis per eq. (3) .

$$\Delta a = -\frac{\Delta\lambda^{\circ}_{AN}}{540\omega_{\oplus}}\sqrt{\frac{\mu}{a}} = -1080.786 \text{ m} \tag{12}$$

The starting estimate of the baseline patrol orbit semimajor axis compensated for J_2 gravity is

$$a = 42164172.921 + 522.25 - 1080.786 = 42163614.385 \text{ m} \tag{13}$$

4.2. East-West Station Keeping

The patrol orbit is eccentric and its orbit track is dependent on the argument of perigee ω. The change in ω over time must be understood and compensated for to maintain the zone of longitudes covered by the orbit. This east-west station keeping differs from traditional methods in which the east-west perturbations arise primarily from the C_{22} and S_{22} gravity coefficients [1, 8]. The first-order secular rate of the argument of perigee due to J_2 gravity is [7]

$$\frac{d\omega}{dt} = \frac{3nC_{20}R_E^2}{4(1-e^2)^2a^2}\left(1 - 5\cos^2 i\right) = 0.0276583 \text{ deg/rev} \tag{14}$$

The effect on longitude coverage due to changing ω is shown in Fig. 11a for the baseline patrol orbit with $\lambda_{AN} = 10°$. The maximum (eastern most) longitude of $40°$ occurs, by design, for $\omega \approx 90°$. Fig. 11b shows the oblique view in ECEF coordinates of the multiple patrol orbits of Fig. 11a. Fig. 11c shows the "top" view (looking in the $-\hat{z}$ direction) of the same orbits. Changing ω clearly results in different patrol orbits that do not enclose the same patrol zone. The secular change in ω described by (14) will therefore result in an east-west shift in the longitudes covered by the patrol orbit. Fig. 12 demonstrates that the longitude of the ascending node λ_{AN} can be changed to make the various orbit track longitudes align very well. There is some latitude dispersion between the different orbits (Fig. 12b, shown larger in Fig. 10), but the same patrol zone is covered almost identically in the longitude and radial dimensions (Figs. 12a and 12c).

The longitude of the ascending node will need to vary at a rate different from the rate of change of argument of perigee. The required rate could be determined empirically from precision numerical integration over long periods of time. If a mean rate can be found that is suitable for the entire planned spacecraft lifetime, then very minimal (if any) east-west station keeping for gravity perturbations would be required.

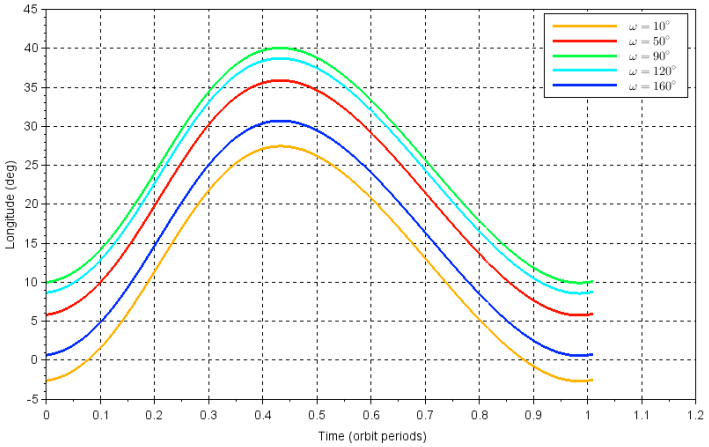

(a) Longitude coverage.

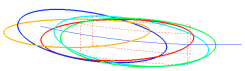

(b) Oblique view.

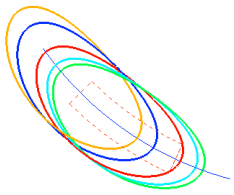

(c) Top view.

Fig. 11: Multiple patrol orbits: different ω, same λ_{AN}.

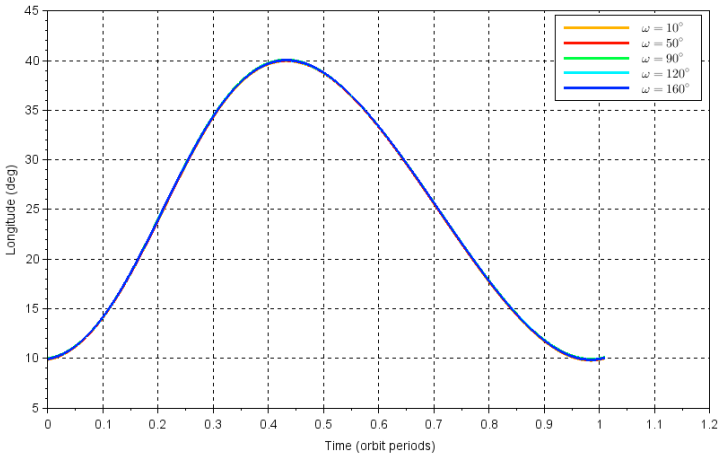

(a) Longitude variation.

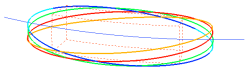

(b) Oblique view.

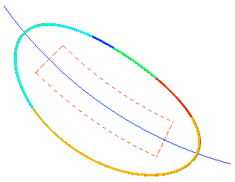

(c) Top view.

Fig. 12: Multiple patrol orbits: different ω, different λ_{AN}. A larger view of (b) is shown in Fig. 10.

4.3. Inclination Drift

The patrol orbit inclination will drift in a manner similar to the traditional geo orbit in most cases. This is primarily due to the third-body gravitational forces of the sun and moon [1]. The actual change in inclination over time will be affected by the initial orbit insertion conditions and the date and time of insertion. Left uncontrolled, typical inclination drift rates are between $0.75°$ and $0.95°$ per year on a 55 year cycle with maximum inclination of approximately $15°$ [8]. Inclination station keeping for a traditional geo orbit is commonly handled by carefully choosing the orbital initial conditions and/or performing plane change maneuvers after the inclination has built up to some predetermined level. A total velocity change of approximately 50 m/s per year is required to compensate for all inclination drift. Because the patrol orbit will not be broadcasting signals to multiple users on the ground, it may be acceptable to allow the inclination to drift to any value with no (or minimal) station keeping maneuvers performed over the spacecraft lifetime.

4.4. Eccentricity Drift

The eccentricity gives the patrol orbit its east-west longitudinal variation, and can be expected to vary over time due to perturbations. There is no secular change in eccentricity due to J_2 gravity. However, the long-period rate of change in eccentricity due to J_3 gravity (i.e., "pear shaped Earth") can be derived using Kaula's method to be [7]

$$\frac{de}{dt} = -\frac{3}{2}\frac{nR_E^3 C_{30}}{ap^2}\cos\omega \sin i \left(\frac{5}{4}\sin^2 i - 1\right) \tag{15}$$

where $p = a(1-e^2)$, and $C_{30} = -J_3$. Because $\cos\omega = 0$ for $\omega = 90°$, the equation is zero for the baseline patrol orbit. Therefore, the secular and long-period rates of change in eccentricity due to two dominant gravitational effects are both zero. Again, this makes $\omega = 90°$ a good default choice for argument of perigee of a patrol orbit. As with inclination drift, high-fidelity numerical studies could be performed to ascertain an accurate model of the effect of perturbations on the eccentricity.

5. MANEUVERING

In addition to any station keeping maneuvers, it is important to understand the requirements and capabilities of general maneuvering in relation to patrol orbits. This section explores the first-order Δv requirements for basic maneuvers

as well as orbit insertion and disposal requirements. The Δv requirements for initiating a synchronous, coplanar "boomerang" orbit are also presented.

5.1. Longitude Drift

The longitude of the ascending node of a patrol orbit may need to be changed over the course of the mission lifetime. Reasons for this might include orbit insertion, station keeping requirements, or change of mission. The change in velocity of a nominal geo orbit to initiate a constant longitude drift at a rate of $\dot{\lambda}$ rad/sec is [8]

$$\boxed{\Delta v \text{ (longitude drift)} = \frac{r\dot{\lambda}}{3} \approx 2.85 \text{ m/s per deg/day}} \tag{16}$$

where $\dot{\lambda} = 2.02 \times 10^{-7}$ rad/sec $= 1$ deg/day. The function is very linear near geo altitudes. For example, a 2 deg/day longitude drift would require ≈ 5.7 m/s. Equation (16) is a good first-order estimate of the Δv required to drift from a nominal geo parking orbit to the ascending node of a patrol orbit. If the longitude drift is to be halted, the same Δv will need to be applied again at the terminal point in the orbit.

5.2. Plane Change

A simple plane change may be required to change the inclination or the ascending node of the patrol orbit. At nominal geo altitude, the orbital velocity is $v = (\mu\omega_{\oplus})^{1/3} = 3074.660$ m/s, and the required Δv for a simple plane change is

$$\boxed{\Delta v \text{ (plane change)} = 2v \sin(\Delta i/2) \approx 53.66 \text{ m/s per deg}} \tag{17}$$

5.3. Orbit Insertion

To understand the velocity requirements for insertion into the baseline patrol orbit, a comparison can be made to a nominal geosynchronous orbit by computing the Δv requirements to transfer from the nominal orbit to the patrol orbit. No optimization is applied – these are simply first-order computations of one possible sequence of insertion maneuvers for approximate comparison to the nominal geo orbit.

The maneuver sequence begins by assuming the spacecraft is in a nominal geo orbit, and is located at the desired longitude of the ascending node of the patrol orbit. Lambert targeting (e.g. [9, 5]) is used to target from the ascending node to the patrol orbit apogee point with transfer time such that the spacecraft will arrive at apogee at the time it would have had it already been on the patrol orbit. The pre-maneuver ECI initial conditions (orbital state) at the ascending node are

$$\begin{aligned} \bar{r}_{AN} &= (-20186085.299, 37018096.094, 0.000) \text{ m} \\ \bar{v}_{AN} &= (-2699.402, -1471.993, 0.000) \text{ m/s} \end{aligned} \tag{18}$$

The baseline patrol orbit ECI initial conditions at apogee are

$$\begin{aligned} \bar{r}_a &= (41852232.528, 22822154.261, -1664684.507) \text{ m} \\ r_a &= |\bar{r}_a| = 47699384.348 \text{ m (5535 km above geo belt altitude)} \\ \bar{v}_a &= (-1289.916, 2365.503, 0.000) \text{ m/s} \end{aligned} \tag{19}$$

The time flight from the ascending node to apogee is $(17950.858 + 43082.050) = 61032.908$ sec. (computed using Kepler's equation). The velocity required (post maneuver) at the ascending node is

$$\bar{v}_{AN} \text{ (required)} = (-2491.379, -1807.913, 106.608) \text{ m/s} \tag{20}$$

The velocity upon arrival at apogee is

$$\bar{v}_a \text{ (arrival)} = (-1257.608, 2389.824, -1.397) \text{ m/s} \tag{21}$$

Lambert targeting is again applied to maneuver from apogee to the perigee point of the patrol orbit with a time of flight of 43082.050 sec (1/2 patrol orbit period). Because transferring from apogee to perigee is a 180° transfer, special precautions may be necessary to ensure the Lambert targeting routine is capable of computing the required Δv (e.g., [10]). The patrol orbit ECI initial conditions at perigee are

$$\begin{aligned} \bar{r}_p &= (-32138858.918, -17525422.508, 1278332.321) \text{ m} \\ r_p &= |\bar{r}_p| = 36628961.494 \text{ m (5535 km below geo belt altitude)} \\ \bar{v}_p &= (1679.767, -3080.432, 0.000) \text{ m/s} \end{aligned} \tag{22}$$

The resulting Δv for this particular sequence of maneuvers is

$$\boxed{\begin{aligned} \Delta v \text{ (AN to apogee)} &= 409.245 \text{ m/s} \\ \Delta v \text{ (apogee to perigee)} &= 40.463 \text{ m/s} \\ \Delta v \text{ (total)} &= 449.708 \text{ m/s} \end{aligned}} \tag{23}$$

For comparison, if there was no plane change required (i.e., the initial geo orbit was inclined $i = 2^\circ$), the total velocity change required by this sequence of maneuvers would be 395.017 m/s. These Δv requirements are probably higher than what would be expected to be delivered by the patrol orbit spacecraft. In such cases, the booster (launch and ascent vehicle) and/or an upper stage would be required to deliver the necessary velocity to insert the spacecraft into the patrol orbit.

5.4. Asynchronous Drift

To initiate an asynchronous longitude drift of the patrol orbit, the semimajor axis (a) must be changed to achieve the proper orbital timing relative to the rotating Earth. The necessary change in a can be estimated from (3). The amount of Δv to effect Δa is derived from the Gaussian form of the variation of parameters equation for the semimajor axis [8]

$$\Delta a = \frac{2a^2}{h} \left[e \sin \nu \Delta v_r + (1 + e \cos \nu) \Delta v_\nu \right] \tag{24}$$

where h is specific angular momentum, $h = \sqrt{\mu a (1 - e^2)}$. By, constraining the maneuver to occur at perigee $(\nu = 0^\circ)$ the equation becomes

$$\Delta a = \frac{2a^2}{h} (1 + e) \Delta v \tag{25}$$

Substituting (3) into the equation for Δa and solving for Δv yields

$$\Delta v = -\frac{\Delta \lambda^\circ_{AN}}{1080 \omega_\oplus} \frac{\mu \sqrt{1 - e^2}}{a^2 (1 + e)} \tag{26}$$

An example asynchronous patrol orbit with a longitude drift rate of $+5^\circ$ (east) per day is shown in Fig. 13. In this case, the Δv required to initiate the drift from the baseline patrol orbit was -12.474 m/s.

5.5. Disposal

Near the end of its useful lifetime, the patrol orbit spacecraft can be moved to a "disposal" orbit where it will not interfere with other patrol orbits or nominal geo belt orbits. A disposal orbit with perigee 250 km higher than the geo belt altitude is commonly used [11]. The required Δv can be computed using the *vis-viva integral* of astrodynamics [9]

$$v^2 = \mu \left(\frac{2}{r} - \frac{1}{a} \right) \tag{27}$$

where $r = r_a$ and $a = (r_a + r_{geo} + 250000)/2 = 45056778.634$ m. The velocity required at the apogee point will be 2804.710 m/s. The required change in velocity is

$$\boxed{\Delta v \text{ (raise perigee)} = (2804.710 - 2694.343) = 110.367 \text{ m/s}} \tag{28}$$

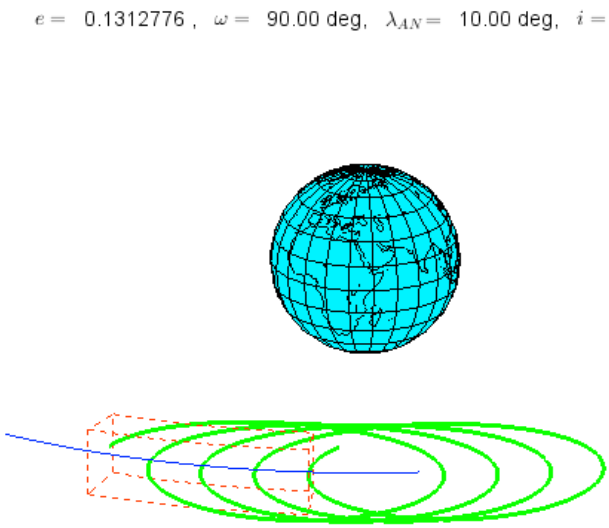

Fig. 13: Asynchronous patrol orbit: $\Delta\lambda_{AN} \approx +5^\circ$ (east) per day, 4 day orbit track shown.

For reference, the Δv required to transfer from a nominal geo orbit to a 250 km higher circular orbit is ≈ 9.075 m/s.

An alternate disposal scheme might be to circularize at apogee altitude, $a = r_a = 47699384.348$ m. The velocity required will be 2890.763 m/s, for a required change in velocity of 196.420 m/s. The resulting altitude will be ≈ 5535 km above the nominal geo belt, greatly exceeding the 250 km guideline, but probably not worth the additional propellant required.

The +250km guideline might not be appropriate for patrol orbit disposal. Long-term studies are required to determine suitable alternatives. It might be acceptable to simply leave the spacecraft in the patrol orbit since it will naturally not interfere with geo orbits. Another alternative might be to raise apogee by 250 km and raise or lower perigee by 250 km. The type of disposal orbit would not interfere with geo orbits or other nominal patrol orbits.

5.6. Boomerang Flyby

A particular patrol orbit mission may require a sub-satellite (e.g., a CubeSat) to fly through the patrol zone to perform a relatively close flyby of an RSO for imaging or inspection, then return to rendezvous with the primary spacecraft in the patrol orbit. A flyby trajectory can be designed to pass through a target point on or near the geo belt in the patrol zone (i.e., a point near the RSO at a specified range), and be geosynchronous and coplanar with the patrol orbit. The coplanar flyby orbit requires minimal velocity change to initiate, and presents favorable in-plane departure and rendezvous conditions (e.g., no cross-track motion). The sub-satellite will be on a "free return" trajectory to rendezvous with the primary spacecraft after one orbital period with no further maneuvering required. Such a synchronous, coplanar trajectory is referred to as a "boomerang" flyby orbit. It should be noted that with a constrained boomerang flyby orbit the time of closest approach to the target RSO cannot be independently specified. However, the time of closest approach is computed during the trajectory design process.

A target point in the equatorial plane, on or near the geo belt and in the vicinity of the RSO to be inspected is selected based on range, solar phase angle during the flyby, face(s) of the RSO to be imaged, etc. Because the boomerang orbit is to be coplanar with the patrol orbit, the time when the target point will be at the longitude of the descending node must be determined (the ascending node case will be considered next). Begin with the patrol orbit spacecraft at the ascending node. This will be the initial estimate of the epoch time $(t = 0)$ for the boomerang orbit. The wait time for the target point to arrive at the longitude of the descending node is (working in radians)

$$\Delta t = \frac{\pi - \Delta\lambda}{\omega_\oplus} \text{ sec} \tag{29}$$

This will also be the initial guess at the boomerang time of flight from the patrol orbit to the target point at the descending node. The target point position vector in ECI coordinates will be

$$\bar{r}_2 = r_2 \begin{bmatrix} \cos(\Omega + \pi) \\ \sin(\Omega + \pi) \\ 0 \end{bmatrix} \tag{30}$$

where r_2 is the target point radial distance, and Ω is the RA of the ascending node of the patrol orbit. To pass through a target point on the geo belt, r_2 will equal the nominal geo radius from (1). With the target point known, Lambert targeting (cf. [9, 5]) is applied to determine the velocity required to transfer from the patrol orbit ascending node $(\bar{r}_1)$ to the target point $(\bar{r}_2)$ in the time of flight determined from (29). This will be a 180° transfer, so proper numerical safeguards must be made when performing the Lambert targeting (cf. [10]). The Lambert targeting routine will return the required initial velocity vector $\bar{v}_1$, from which the semimajor axis of the transfer orbit can be computed.

$$a_{\text{TX}} = \left(\frac{2}{r_1} - \frac{v_1^2}{\mu} \right)^{-1} \tag{31}$$

By design, the boomerang orbit must be geosynchronous. If a_{TX} does not equal the nominal geosynchronous value a_{nom}, then the transfer time of flight is changed by a small amount: longer if $a_{\text{TX}} < a_{nom}$, shorter if $a_{\text{TX}} > a_{nom}$. The final target point $\bar{r}_2$ does not change, but the initial point $\bar{r}_1$ on the patrol orbit must be changed to correspond to the new time of flight. The initial point is numerically propagated forward or backward in time by the *change* in time of flight to determine the new departure point $\bar{r}_1$. Lambert targeting is applied again, and the new a_{TX} checked against a_{nom}. The process is repeated using numerical methods (e.g., *regula falsi*) until $a_{\text{TX}} = a_{nom}$ within some small tolerance. When the solution is converged upon, the boomerang flyby transfer orbit computed from the Lambert targeting routine will be coplanar and geosynchronous, causing the flyby spacecraft to depart from the patrol orbit spacecraft at the epoch time, pass through the flyby target point at the predicted time, and return to rendezvous with the patrol orbit spacecraft after one orbital period.

It may be more propellant efficient to pass through the target point at the ascending node instead of the descending node. In that case the transfer orbit will originate near the descending node on the eastern end of the patrol zone, and the wait time for the target to arrive at the ascending node will be

$$\Delta t = \frac{\pi + \Delta\lambda_N - \Delta\lambda}{\omega_\oplus} \tag{32}$$

The Δv required to pass through a target point from the baseline patrol orbit is shown in Fig.14. The descending Δv requirements are shown in red, and the ascending requirements are shown in green. The cross-over point, where it becomes more propellant efficient to use the other type of flyby, occurs very near the middle of the patrol zone at $\Delta\lambda \approx 15^\circ$.

The orbital elements for three example boomerang flybys (two descending and one ascending) launched from the baseline patrol orbit are listed in Table 2. The orbits can be easily recreated, verified, and experimented with in a two-body astrodynamics simulation environment. The target point for the $\Delta\lambda = 15^\circ$ descending case is $1,000$ km below the nominal geo belt altitude, demonstrating that flyby target points do not need to be located on the geo belt. Note that a, i, and Ω are the same for all three boomerang orbits, indicating that each orbit is geosynchronous and coplanar with the baseline patrol orbit (cf. Table 1). Also listed in Table 2 are the times of flight (Δt) from the launch points to the target points. The three example boomerang trajectories are illustrated in Fig. 15. All three orbits are geosynchronous and coplanar with the patrol orbit in inertial space, although this is not apparent in the Earth-fixed view of the figure.

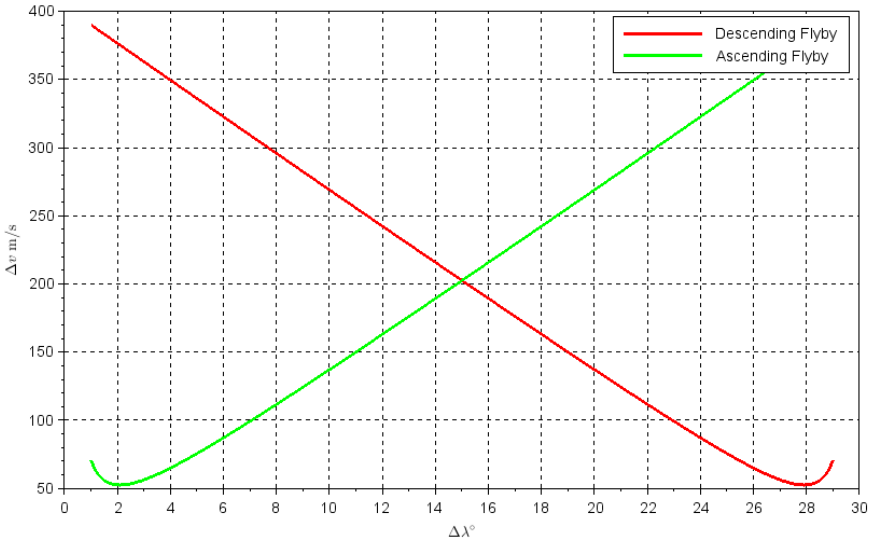

Fig. 14: $30° \times 4°$ baseline patrol orbit boomerang flyby Δv requirements.

Table 2: Example boomerang flyby parameters: Δr is target altitude relative to geo belt, Δt is time between departure from patrol orbit and target arrival, t_{tgt} is target arrival time, t_{rndz} is rendezvous time with patrol orbit (defined in Table 1).

	$\Delta\lambda = 20°$, descending $\Delta r = 0$ km	$\Delta\lambda = 15°$, descending $\Delta r = -1,000$ km	$\Delta\lambda = 10°$, ascending $\Delta\lambda = 10°$km, asc
Epoch	20170710 11:49:55.468	20170710 10:07:27.270	20170710 22:08:26.249
a	42164172.921 m	42164172.921 m	42164172.921 m
e	0.087682	0.071282	0.087682
i	2.000000°	2.000000°	2.000000°
Ω	118.603775°	118.603775°	118.603775°
ω	84.969752°	105.532476°	95.030248°
ν	272.453045°	227.278347°	87.546955°
Δv	137.176 m/s	201.545 m/s	137.176 m/s
Δt	38899.688 sec	46244.609 sec	47264.413 sec
t_{tgt}	20170710 22:38:15.156	20170710 22:58:11.879	20170711 11:16:10.661
t_{rndz}	20170711 11:45:59.568	20170711 10:03:31.370	20170711 22:04:30.349

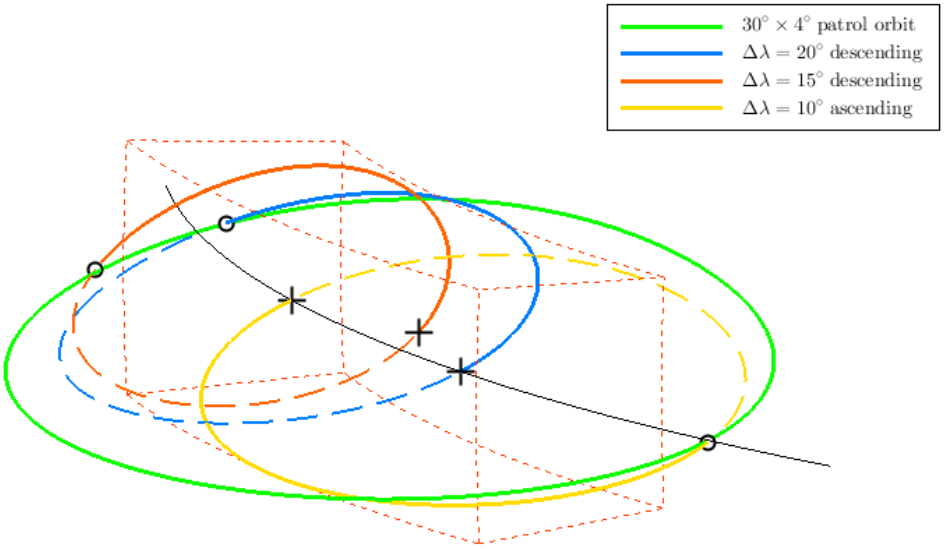

Fig. 15: Example coplanar, geosynchronous boomerang trajectories in ECEF. All relative motion is clockwise in this view. Outbound segments shown solid; inbound segments shown dashed. Departure/rendezvous points are circles; target points are crosses. For reference, the patrol zone (small red dashes) spans 20° longitude (15° to 35° from left to right).

6. PATROL ORBIT USING SIERRA NEVADA CORPORATION SN-200G SPACECRAFT

The Sierra Nevada Corporation SN-200G microsat spacecraft was developed for low-cost geosynchronous missions, leveraging new and emerging direct-inject launch options and Evolved Expendable Launch Vehicle (EELV) Secondary Payload Adapter (ESPA) compatibility. The design supports moderately sized payloads, including sufficient mass, power, pointing performance and platform stability needed for imaging missions. Although the spacecraft has insufficient propulsion capability on its own for GTO -GEO transfer, the propulsion systems green propellant is preserved to provide significant delta V for GEO orbit maneuvers. Redundant avionics and subsystems were developed to ensure long life and successful end-of-mission disposal. Fig. 16 and Fig. 17 describe the SN-200G layout.

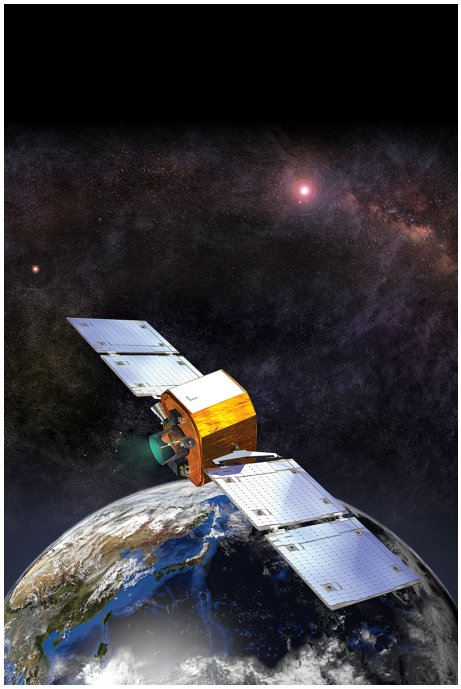

Fig. 16: SN-200G developed to accommodate multiple payloads to GEO patrol orbit.

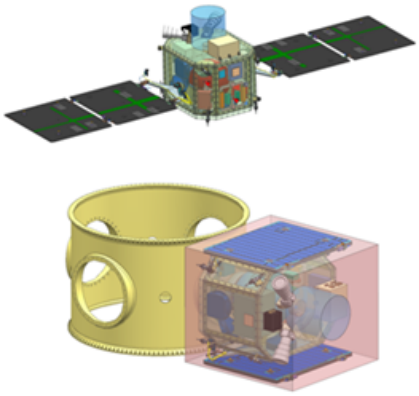

Fig. 17: SN-200G rideshares to GEO using ESPA Grande or other alternatives.

6.1. Delta-V: station keeping, maneuvering, disposal

A delta-V budget for a geo patrol orbit was created to preserve considerable mission flexibility and maneuverability (shown in Table 3). This budget assumes satellite deployment from the launch vehicle in an equatorial geostationary orbit, maneuver adjustment to the initial patrol orbit, and orbit maintenance and adjustments throughout a 5 year mission. Sufficient propellant is reserved for End of Mission (EOM) placement to the internationally agreed geo disposal altitude.

Table 3: Δv budget, 5 year mission.

	Δv (m/s)	Comment
Patrol Orbit Station Keeping		
East-West	0	mission dependent
Inclination Drift	0	mission dependent
Eccentricity Drift	0	mission dependent
Other Station Keeping	50	mission dependent
Maneuvering		
Longitude Drift	23	5.7 m/s for 2 deg/day
Plane Change	0	53.7 m/s per degree, LV supplied
Final Orbit Insertion	40.4	410 m/s, LV supplied
Asynchronous Drift	50	4 starts/stops, 5 deg/day
EOM Disposal	110.4	Perigee 250 km above geo belt
Total	273.8	
SN-200G Capability	350	

The SN-200G design accommodates payloads for a variety of missions including refueling, repair, and servicing of existing geo spacecraft, and imaging for space situational awareness or space debris assessment and removal missions (see Table 4). Three-axis stabilization is achieved with reaction wheels, and 12 coupled thrusters support proximity operations if required. Precision attitude control is achieved using blended star tracker, IMU and GPS solutions.

The SN-200G spacecraft is engineered to provide a stable imaging platform including a number of features that have been flight proven to provide stability and minimize vehicle jitter. Other spacecraft characteristics are designed to lower cost in a multi-unit production environment, including primary structure access points and modular design of payload, propulsion, and avionics modules.

The SN-200G spacecraft includes redundancy commensurate with a 5 year mission life and responsible end-of-mission disposal. Redundant flight computer, power avionics, propulsion, and attitude control is included. Reliability is enhanced through safe mode features and a robust fault protection system.

7. SUMMARY AND CONCLUSION

In this paper it has been shown that introducing eccentricity to a geosynchronous orbit produces both radial and longitudinal variations in the orbit track. The result is periodic, quasi-elliptical relative motion around a fixed segment of the geo belt when viewed in Earth-fixed coordinates. The size of the relative motion (quasi-ellipse) is determined by the amount of eccentricity in the orbit, and incorporating orbit inclination can lead to an even wider range of relative motion. Because a spacecraft in this type of orbit remains in the vicinity of a fixed portion of the geo belt with continuous relative motion, this type of orbit is called a *patrol orbit*. The volume of space around the geo belt that the patrol orbit is responsible for is called the *patrol zone*.

The natural (no thrusting required) relative motion of a patrol orbit offers several advantages for certain geo missions including space situational awareness (SSA). The patrol orbit does not occupy a slot in the geo belt, and it crosses the equator at an altitude different than the geo belt altitude, significantly reducing collision hazard and interference issues including the case of loss of control of the patrol orbit spacecraft. The patrol orbit guarantees that objects in the patrol

Table 4: SN-200G specifications.

Parameter	Spacecraft Capability
Maximum Payload Mass	150 kg
Maximum Payload Power	500 W Orbit Average
Maximum Payload Data Rate	100 Mbps
Maximum Payload Volume	100 cm x 100 cm payload deck; height limited by LV fairing
Maximum Payload Data Storage	96 GBytes
Pointing Knowledge	$< 0.005^\circ, 3\sigma$ all axes
Pointing Control	$0.01^\circ, 3\sigma$ all axes
Pointing Stability	Payload dependent
Slew Rate	Typically > 1 deg/sec, payload mass prop's dependent
Compatible LVs	All LVs with direct to GEO capability, ESPA Grande port
Compatible Orbits	GEO and near-GEO
Propellant Mass	55 kg (> 350 m/s Δv with 150 kg P/L)
Spacecraft Body Mass (dry)	155 kg, 200 kg with full redundancy
Spacecraft Bus Power	Generation: 770 W peak (≈ 210 W avg. bus loads)
Comm Up/Downlink Band	S/X/Ka
Structure	Aluminum honeycomb
Heritage Mission	TacSat-2, DSX
Nominal Schedule	30 months bus delivery

zone will always be within a specified, designed range, meeting sensor operational requirements. The relative motion of the patrol orbit over time provides improved viewing geometry (angular diversity) compared to geostationary and simple inclined geo orbits. It also provides daily varying points of view of RSO's of interest that a fixed geo orbit cannot provide. Observation of RSO's from a patrol orbit is not restricted to nighttime viewing only and is not subject to weather conditions as Earth-based sensors are. The patrol orbit can also be made asynchronous to cover the entire geo belt over a desired number of revolutions.

Using an example patrol orbit as a baseline, the basic equations and methods for determining specific patrol orbit parameters were presented. It was found that a patrol orbit with argument of perigee $\omega = 90^\circ$ has several advantages, but it is not the only possible patrol orbit. A first-order analysis of station keeping requirements of the baseline patrol orbit showed that it may be possible to avoid station keeping entirely (or nearly so) by diligently selecting the initial orbital conditions and allowing for reasonable latitude and longitude margins.

Basic maneuver analysis showed that additional Δv compared to a typical geo orbit is required to establish the patrol orbit. Ideally, the required insertion velocity should be provided by the ascent vehicle (booster), leaving the greatest amount of propellant onboard the spacecraft to perform mission essential and disposal maneuvers. The disposal Δv requirements were higher than for a typical geo orbit. However, there might exist better disposal orbits for patrol orbits requiring significantly less Δv than the typical geo orbit. The design of a coplanar, synchronous boomerang trajectory useful for close inspection and imaging flybys was presented. An analysis of a currently available spacecraft (Sierra Nevada Corporation SN-200G) for use in a patrol orbit was also presented.

This paper represents the preliminary investigation of the patrol orbit. Future research to be done includes investigation of the use of rendezvous and proximity operations techniques for application to patrol orbits, optimization of maneuvering in and around the patrol zone, maneuvering with low-thrust systems such as electric propulsion, and high-fidelity long-term investigation of perturbations and station keeping requirements. Constellations of multiple patrol orbits and multiple spacecraft phased in the same patrol orbit also deserve further study. Other future research might include exploitation of the unique tracks of patrol orbits for improved space-to-space and space-to-ground communications as well as the possible advantages offered to Earth observing missions.

References

[1] Soop, E.M., *Handbook of Geostationary Orbits*, Springer Science+Business Media, Dordrecht, 1994.

[2] Fehse, W., *Automated Rendezvous and Docking of Spacecraft*, Cambridge University Press, 2003.

[3] Space-Track.org, Joint Functional Component Command for Space (JFCC SPACE), US Air Force, https://www.space-track.org

[4] Tapley, B., Schutz, B., Born, G., *Statistical Orbit Determination*, Elsevier Academic Press, Amsterdam, 2004.

[5] Vallado, D., *Fundamentals of Astrodynamics and Applications*, 4th ed., Microcosm Press, Hawthorne, California, 2013.

[6] Gottlieb, R., Thompson, B. , Bisected Direct Quadratic Regula Falsi, *Applied Mathematical Sciences*, Vol. 4, No. 15, 2010, pp.709-718.

[7] Kaula, W.M., *Theory of Satellite Geodesy: Applications of Satellites to Geodesy*, Dover Publications, Inc., Mineola, New York, 2000.

[8] Pritchard, W.L., Suyderhoud, H.G., Nelson, R.A., *Satellite Communication Systems Engineering*, 2nd ed., Prentice Hall, Englewood Cliffs, New Jersey, 1993.

[9] Battin, R. H., *An Introduction to the Mathematics and Methods of Astrodynamics*, AIAA Education Series, American Institute of Aeronautics and Astronautics, Inc., New York, 1987.

[10] Thompson, B., Enhancing Lambert Targeting Methods to Accommodate 180-Degree Transfers, *Journal of Guidance, Control, and Dynamics*, Vol. 34, No. 6, 2011, pp.1925-1929.

[11] Walls, R.L., Gaylor, D., Vishnu, R., Furfaro, R., Jah, M., Assessing the IADC Space Debris Mitigation Guidelines: A case for ontology-based data management, *Advanced Maui Optical and Space Surveillance Technologies Conference (AMOS)*, 2016.